



# Capturing the Mechanical Unfolding Pathway of a Large Protein with Coiled-Coil Probes\*\*

Qing Li, Zackary N. Scholl, and Piotr E. Marszalek\*

**Abstract:** The folding behaviors and mechanisms of large multidomain proteins have remained largely uncharacterized, primarily because of the lack of appropriate research methods. To address these limitations, novel mechanical folding probes have been developed that are based on antiparallel coiled-coil polypeptides. Such probes can be conveniently inserted at the DNA level, at different positions within the protein of interest where they minimally disturb the host protein structure. During single-molecule force spectroscopy measurements, the forced unfolding of the probe captures the progress of the unfolding front through the host protein structure. This novel approach allows unfolding pathways of large proteins to be directly identified. As an example, this probe was used in a large multidomain protein with ten identical ankyrin repeats, and the unfolding pathway, its direction, and the order of sequential unfolding were unequivocally and precisely determined. This development facilitates the examination of the folding pathways of large proteins, which are predominant in the proteasomes of all organisms, but have thus far eluded study because of the technical limitations encountered when using traditional techniques.

Significant progress has been made over the last 50 years towards the understanding of how small single-domain proteins fold into their 3D structures<sup>[1]</sup> or misfold into aggregation-prone conformations.<sup>[2]</sup> However, much less is known about the folding mechanisms of large multidomain proteins, which dominate the proteasome in all kingdoms of life (approximately 62% of all proteins in a set of 358 complete genomes have 2–5 domains).<sup>[3]</sup> Recent work has shown that large proteins have evolved specialized energy landscapes that may reduce misfolding through a number of mechanisms.<sup>[4–7]</sup> However, the research on the folding of multidomain proteins is still in its infancy, partially because of the lack of appropriate experimental methods that would

allow the study of the unfolding and refolding of very large polypeptides while avoiding their aggregation and misfolding.<sup>[3,6,8]</sup>

Single-molecule force spectroscopy (SMFS) is useful for investigating protein folding outside the perturbation of strictly mechanical proteins [e.g., Ref. [8a,d,9,17]], and has unique advantages for studying large multidomain proteins as SMFS examines individual proteins one by one under conditions minimizing their possible aggregation. Equally importantly, SMFS may apply denaturing forces to almost any arbitrary fragment of a protein<sup>[10]</sup> and examine the effect of this perturbation on the remaining parts of the protein and thus allows the direct examination of the coupling of domains and the folding cooperativity.<sup>[8a]</sup> However, multidomain proteins present a problem for interpreting SMFS data: The domain that gives rise to a signal (force peak) must be identified out of the multiple domains in the protein. Some methods exist to determine domains by SMFS on multidomain proteins using truncation,<sup>[11]</sup> contour length increments,<sup>[8,12]</sup> disulfide bond cross-linking,<sup>[8b,11]</sup> or modifications by ligand binding.<sup>[13]</sup> However, there is still a need for new methods that can probe multidomain proteins when the aforementioned approaches are not applicable (e.g., when many domains are present or when the domains are of a similar size).

Herein, we describe an approach that can precisely report the structural origin of a signal detected by SMFS measurements. In a nutshell, an antiparallel coiled coil (CC) sequence is inserted at the DNA level at various positions within a large multidomain protein and functions as a mechanical probe that can report on the folding status of the surrounding structure when interrogated by SMFS. This idea was inspired by the observation that coiled-coil motifs within various proteins<sup>[14]</sup> tend to be structurally independent from the host and by recent SMFS measurements on coiled coils that revealed their robust mechanical unfolding and refolding properties.<sup>[15]</sup> These two facts combined suggest that a coiled coil inserted at a suitable position within the host protein will not significantly affect the tertiary structure of the target protein, and its characteristic atomic force microscopy (AFM) unfolding pattern will enable the assignment of force peaks to structural elements when the unfolding process passes through the location of the CC probe. Recently, Chwastyk et al.<sup>[16]</sup> also applied a similar strategy to identify SMFS force peaks by inserting a guest protein into a host protein, suggesting the possibility of having an independent polypeptide chain within a host protein without causing the host protein to misfold.

In a recent study, we combined AFM-SMFS with molecular dynamics simulations to examine the unfolding pathway

[\*] Q. Li, Prof. P. E. Marszalek  
Department of Mechanical Engineering and Material Sciences  
Duke University  
Durham, NC, 27708 (USA)  
E-mail: pemar@duke.edu

Z. N. Scholl  
Program in Computational Biology and Bioinformatics  
Duke University  
Durham, NC, 27708 (USA)

[\*\*] We thank Prof. J. Clarke (University of Cambridge, UK) for providing polyI27 plasmids. This work was supported by the NSF (MCB-1052208 to P.E.M.). P.E.M. also acknowledges kind support from the Kimberly–Clark Corporation.

Supporting information for this article is available on the WWW under <http://dx.doi.org/10.1002/anie.201407211>.

of a protein composed of eight consensus ankyrin repeats, NI<sub>6</sub>C.<sup>[17]</sup> Ankyrin repeat proteins have been found to display unusual mechanical properties and extremely robust mechanical refolding behaviors.<sup>[9b,17,18]</sup> We hypothesized that unlike small proteins that unfold in a two-state fashion, this protein unfolds sequentially, from its C terminus to the N terminus;<sup>[17]</sup> this behavior may be shared by other multi-domain proteins. However, it proved quite challenging to provide experimental evidence verifying this pathway.<sup>[19]</sup> Following the mechanical unfolding study of the I27 domain of titin,<sup>[20]</sup> we inserted an unstructured polypeptide to increase the contour length of one of the repeats, but we failed to obtain repetitive unfolding patterns, possibly because the engineered protein became mechanically unstable. Then, we began our new study with the antiparallel coiled coil from the Archeal Box C/D sRNP Core Protein<sup>[21]</sup> (PDB: 1NT2), whose ends are brought together by the fold to within <1 nm (as determined from the crystal structure), as our folding probe to directly capture the directional, stepwise unfolding of consensus ankyrin repeats.

First, we characterized the unfolding of the CC probe by itself. The CC probe was flanked by three I27 domains of titin (Figure 1a), which serve as pulling handles and as a force spectroscopy reference and fingerprint for the facile identification of single-molecule recordings.<sup>[22,23]</sup> A typical force–extension curve for the (I27)<sub>3</sub>–CC–(I27)<sub>3</sub> construct is shown

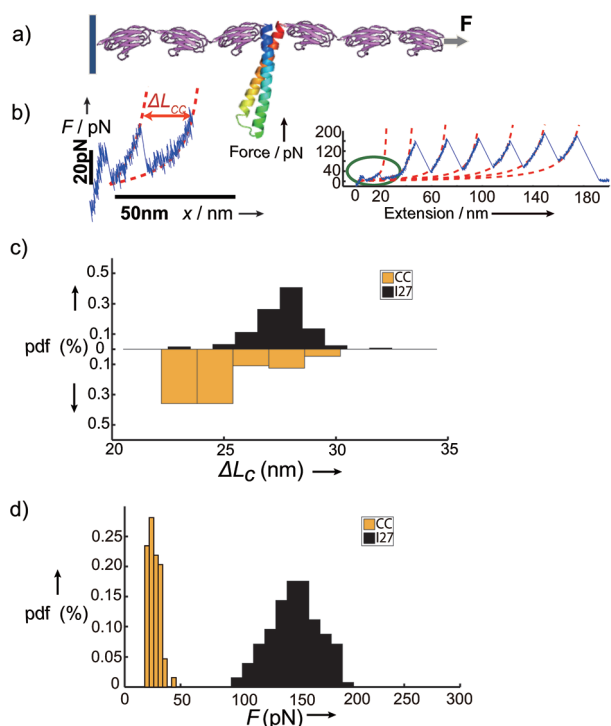


**Figure 1.** AFM force spectroscopy results for the I27<sub>3</sub>–CC–I27<sub>3</sub> construct. a) Schematic representation of the stretching of I27<sub>3</sub>–CC–I27<sub>3</sub>. b) A representative force–extension trace for I27<sub>3</sub>–CC–I27<sub>3</sub>. The inset shows, at higher magnification, the force peak corresponding to the unfolding of the CC structure along with the fits of the worm-like chain model to the data. c) Comparison of the histograms for the contour length increments  $\Delta L_c$  for I27 and CC based on 62 recordings. d) Probability density functions (pdf) for force peaks corresponding to the unfolding of CC and I27.

on the right-hand side in Figure 1b (see also the Supporting Information, Figure S3 for more recordings of this construct). The first peak, with a force of approximately 28 pN at a contour length increment of approximately 26 nm (for a magnified image, see Figure 1b, left), reports an unfolding event of a structure composed of approximately 70 amino acids, as determined by the fits of the worm-like chain (WLC) model of polymer elasticity before and after the peak. The CC probe contains 67 amino acids, so this peak is attributed to the unfolding of the CC structure. The distribution of the contour length increments after the first unfolding peak and the distribution of the contour length increments corresponding to the unfolding of the I27 domains are shown in Figure 1c. In Figure 1d, a histogram of these unfolding forces is shown, which compares them to the unfolding forces corresponding to the I27 domains.

To test the order of events in the unfolding pathway, we used an even bigger protein, NI<sub>10</sub>C, that is composed of 12 ankyrin repeats and contains 385 amino acids. This protein features four additional consensus ankyrin repeats in its core (as compared to NI<sub>6</sub>C).<sup>[17]</sup> The typical unfolding force–extension curve of NI<sub>10</sub>C is shown in Figure 2a, with more recordings superimposed in Figure S4a. The force curve illustrated in Figure 2a is almost the same as that of NI<sub>6</sub>C,<sup>[17]</sup> except for the number of unfolding events, so we expect that our hypothesis of the sequential unfolding of consensus ankyrin repeats also applies to NI<sub>10</sub>C. This view is supported by a coarse-grained steered molecular dynamics simulation (CG-SMD) of NI<sub>10</sub>C, which, similar to NI<sub>6</sub>C, unfolds sequentially from the C to the N terminus (Figure S1a). To directly verify this model, we engineered two protein constructs. (Figure S5). The first construct contains the CC probe towards the N-terminal ankyrin repeat (inserted inside the big loop of the 4th repeat, NI<sub>4</sub>CCI<sub>6</sub>C), and the second construct contains the CC probe towards the C-terminal ankyrin repeat (inserted inside the big loop of the 8th repeat, NI<sub>8</sub>CCI<sub>2</sub>C). Both constructs are flanked by I27 domains for mechanical fingerprinting where four I27 peaks guarantee that the measurement was obtained on a single molecule containing a full-length ankyrin repeat protein.

A typical experimental force–extension curve for NI<sub>8</sub>CCI<sub>2</sub>C unfolding is shown in Figure 2b. The regularly spaced small force peaks below 50 nm extension, with a  $\Delta L_c$  mean value of 10.1 nm and a force peak mean value of 22 pN, correspond to the stepwise unfolding of individual ankyrin repeats.<sup>[17]</sup> They occurred before the bigger peak with an unfolding force of approximately 30 pN and  $\Delta L_c \approx 21$  nm that is absent in the force–extension curve of the host protein, NI<sub>10</sub>C, and therefore likely corresponds to the unzipping of the anti-parallel CC. Over the 130 nm extension regime, the curve displays the characteristic saw-tooth pattern with  $\Delta L_c \approx 28$  nm and force peaks of approximately 157 pN, which is typical of I27 domains at a loading rate of about 120 pNs<sup>-1</sup> (Figure S4b).<sup>[23]</sup> In Figure S4b, we superimposed 15 force–extension recordings of NI<sub>8</sub>CCI<sub>2</sub>C, and they overlap well, showing a consistent position of the CC peak. Figure 2c shows a typical force–extension curve of NI<sub>4</sub>CCI<sub>6</sub>C, which captures the unfolding peak of the CC probe much later than the unfolding of CC in NI<sub>8</sub>CCI<sub>2</sub>C (for a comparison of 15

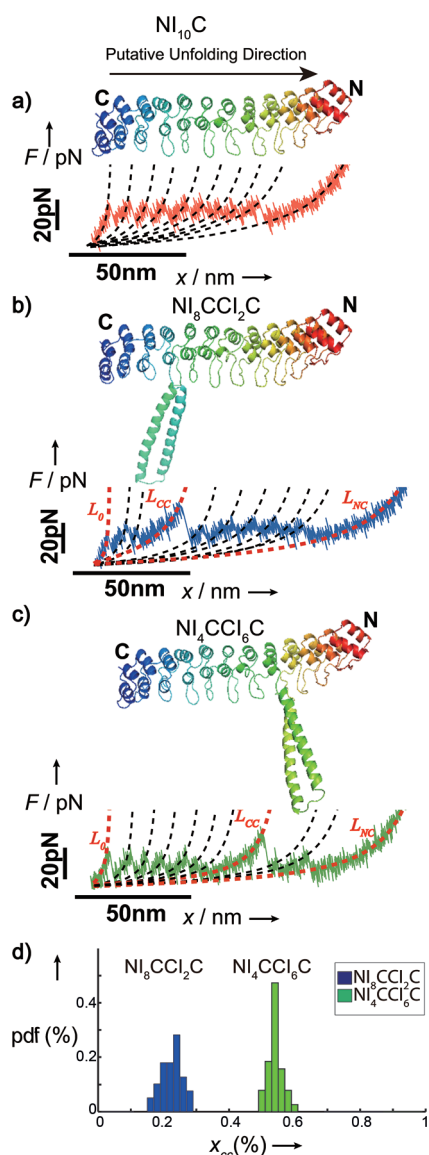


**Figure 2.** The coiled-coil probe reveals the unfolding pathway of  $\text{NI}_{10}\text{C}$ . Three-dimensional structures of a)  $\text{NI}_{10}\text{C}$ , b)  $\text{NI}_8\text{CCI}_2\text{C}$ , and c)  $\text{NI}_4\text{CCI}_6\text{C}$  and their representative force–extension traces. The molecules are oriented so that the C terminus is shown on the left and the N terminus is shown on the right. Solid lines in (a)–(c) display data from SFMS measurements. Dashed lines represent the WLC fitting of each unfolding event.  $L_0$ ,  $L_{\text{CC}}$ , and  $L_{\text{NC}}$  represent the contour lengths in WLC fitting with  $p = 0.6$  nm for each relative part of the curves ( $L_{\text{CC}}$  refers to the length up to the folded CC). d) Comparison of the pdf values of the fractional extension at which the CC unfolds,  $X_{\text{CC}}$ , for the CC values in the unfolding traces of  $\text{NI}_8\text{CCI}_2\text{C}$  and  $\text{NI}_4\text{CCI}_6\text{C}$ .  $X_{\text{CC}} = (L_{\text{CC}} - L_0) / (L_{\text{NC}} - L_0)$ . The protein structures were drawn using visual molecular dynamics<sup>[30]</sup> (VMD) software.

recordings of  $\text{NI}_4\text{CCI}_6\text{C}$ , see Figure S4c). A comparison of Figures S4b and S4c clearly shows the shift of the CC peak towards greater extensions for the  $\text{NI}_4\text{CCI}_6\text{C}$  construct. The absolute extension at which the CC peak occurs depends somewhat on the length of the protein fragment picked up randomly by the AFM tip. To eliminate this variability, we determined the fractional extension at which the CC peak occurred,  $X_{\text{CC}} = (L_{\text{CC}} - L_0) / (L_{\text{NC}} - L_0)$ , for each recording (see

Figure 2 for the definitions of  $L_{\text{CC}}$ ,  $L_0$ , and  $L_{\text{NC}}$ ). The histograms of  $X_{\text{CC}}$  for both constructs are shown in Figure 2d. These results directly show that the CC probe located near the C-terminal ankyrin repeat unfolds at smaller extensions than the CC probe located near the N-terminal ankyrin repeat, which validates our hypothesis, which was based on computer simulations, that the unfolding of consensus ankyrin repeats starts at the C terminus and proceeds in a stepwise fashion to the N terminus.

The unfolding force of the CC probe (Figure 1d) is greater than the unfolding forces of ankyrin repeats in  $\text{NI}_{10}\text{C}$ , yet the coiled coil unfolds according to its placement in  $\text{NI}_8\text{CCI}_2\text{C}$  and  $\text{NI}_4\text{CCI}_6\text{C}$  before the remaining N-terminal ankyrin repeats unfold. This observation seems surprising because typically, mechanically weaker structures unfold before stronger domains. However, the SMD simulations show that the mechanical unfolding of ankyrin repeats is quite complex and involves the forced detachment of individual helices from the stack followed by their unfolding and re-orientation. In simulations, when the unfolding front proceeds to the coiled coil, the coiled coil unfolds first before the helices of the remaining N-terminal repeats start peeling off. This is consistent with our experimental observations (Figure S1b,c). A similar phenomenon of reverse mechanical hierarchy was already observed for other proteins,<sup>[24]</sup> which is an issue worthy of further investigation. In our case, it is possible that whereas the net force measured by the cantilever upon coiled-coil unfolding is greater than the force necessary to unfold the neighboring repeat, the actual component of the net force acting on the neighboring helix is lower than the force needed to peel it off from the stack, and this force then reaches the necessary magnitude only after the CC probe has unfolded and the polypeptide chain has reoriented.

To examine whether the specific placement of the CC probe may affect the interpretation of the unfolding pathway of  $\text{NI}_{10}\text{C}$ , we engineered another construct,  $\text{NI}_7\text{CC}(\text{SL})_2\text{C}$ , in which the CC probe was placed in a small loop connecting the helices in the eighth consensus repeat (Figure S4d). SMFS recordings of  $\text{NI}_7\text{CC}(\text{SL})_2\text{C}$  captured the unfolding of the CC probe; the results are consistent with its placement close to the C terminus and further support our hypothesis that the overall unfolding of  $\text{NI}_{10}\text{C}$  proceeds from the C to the N terminus. We plan to test the generality of the host proteins using the I27 domain of titin as an example of an all- $\beta$  protein, which has been intensively studied by AFM and computer simulations.<sup>[25]</sup> Our approach may be generalized to other multidomain proteins if it is possible to find loop regions or other appropriate elements, such as turns or unstructured segments, that are close to the surface of the proteins and far away from their critical functional sites.

For host proteins that are significantly weaker than our CC probe, the CC probe may not serve as a reference to capture the unfolding pathway as the CC would not unfold until all of the host protein structure has unfolded. In such cases, the design of other CC probes with desired mechanical stabilities might be necessary. In a nutshell, the main advantages of our CC probe are the ability to incorporate it into the host protein at the DNA level, its robust, independent folding, which brings the N and C termini very close to each



other for a minimal disruption of the host protein, and characteristic length and force signatures in force spectrograms of the host protein. The main limitation is that the mechanical resistance of the probe cannot be significantly greater than the resistance of the host structure. However, this limitation can be circumvented by a design of a suite of CC probes with various unfolding forces.

Our results indicate that the unfolding of NI<sub>10</sub>C under one-dimensional geometrical constraints occurs through a sequential vectorial process in the C→N direction. More generally, our studies suggest that coiled-coil peptides, either natural or synthetic peptides designed to display a range of mechanical stabilities, could be very useful for examining the unfolding pathways of large multidomain proteins, which are difficult to study by bulk measurements.

### Experimental Section

**Protein design, engineering, and purification:** The gene sequences of NI<sub>10</sub>C,<sup>[26]</sup> NI<sub>8</sub>CCI<sub>2</sub>C, and NI<sub>4</sub>CCI<sub>6</sub>C were synthesized and cloned into the pUC57 vector by GenScript (Piscataway, NJ, USA) and then inserted into the poly(I27) pRsetA vector.<sup>[27]</sup> All engineered plasmids were transformed into *E. coli* C41(DE3) pLysS cells. Protein expressions were induced by adding isopropyl-β-D-thiogalactopyranoside (IPTG; 0.2 mM); the reaction temperature was lowered to room temperature after the OD<sub>600</sub> value of the cultures exceeded 0.8. All of the proteins that contained the *Strep* tag were purified using the *Strep*-Tactin Sepharose column.

**Single-molecule force spectroscopy by AFM:** All protein samples were diluted once with phosphate-buffered saline (PBS) to a concentration of approximately 30 μM and then incubated on a freshly cleaned gold surface. After 30 minutes of incubation at room temperature, all samples were used for the AFM pulling experiment without further washing. All stretching measurements were carried out on custom-built AFM instruments.<sup>[28]</sup> All samples were picked up by untreated biolever AFM cantilevers with a spring constant (kc) of 5–10 pN nm<sup>-1</sup> (Model: OBL-10, Bruker AFM Probes, Camarillo, CA, USA) at a pulling speed of 20 nms<sup>-1</sup> at room temperature. The spring constant of each cantilever was calibrated in PBS on clean glass substrates using the energy equipartition theorem.<sup>[29]</sup>

**Coarse-grained steered molecular dynamics simulations of NI<sub>10</sub>C, NI<sub>8</sub>CCI<sub>2</sub>C, and NI<sub>4</sub>CCI<sub>6</sub>C:** The initial geometry of NI<sub>10</sub>C was built based on PDB code 2QYJ by root mean square distance (RMSD) fitting<sup>[17,19]</sup> in VMD.<sup>[30]</sup> The NI<sub>8</sub>CCI<sub>2</sub>C and NI<sub>4</sub>CCI<sub>6</sub>C structures were created by inserting the anti-parallel coiled coil into the NI<sub>10</sub>C structure at the positions specified in Figure S5. Equilibrium molecular dynamic (MD) simulations of the NI<sub>10</sub>C, NI<sub>8</sub>CCI<sub>2</sub>C, and NI<sub>4</sub>CCI<sub>6</sub>C structures using the CHARMM<sup>[31]</sup> force field were performed by NAMD.<sup>[32]</sup> The final equilibrated all-atom structure was then used to generate a coarse-grained model using the SMOG server,<sup>[33]</sup> and then probed by steered MD (SMD) simulations<sup>[34]</sup> using GROMACS.<sup>[35]</sup> The C-terminal Cα atoms of the proteins were pulled with a pulling speed of 0.5–2.5 nmns<sup>-1</sup> by an attached spring force with a spring constant of 6–8 pNnm<sup>-1</sup> while the N-terminal Cα atoms were held fixed. Simulations were robust to changes in pulling speed and also robust to switching the pulling direction (fixing the C terminus instead).

Received: July 14, 2014

Revised: September 10, 2014

Published online: October 22, 2014

**Keywords:** coiled coils · multidomain proteins · single-molecule force spectroscopy · protein folding · protein structures

- [1] a) K. A. Dill, J. L. MacCallum, *Science* **2012**, *338*, 1042–1046; b) D. U. Ferreira, S. S. Cho, E. A. Komives, P. G. Wolynes, *J. Mol. Biol.* **2005**, *354*, 679–692; c) A. I. Bartlett, S. E. Radford, *Nat. Struct. Mol. Biol.* **2009**, *16*, 582–588.
- [2] a) C. M. Dobson, *Nature* **2003**, *426*, 884–890; b) P. L. Clark, *Trends Biochem. Sci.* **2004**, *29*, 527–534.
- [3] J. H. Han, S. Batey, A. A. Nickson, S. A. Teichmann, J. Clarke, *Nat. Rev. Mol. Cell Biol.* **2007**, *8*, 319–330.
- [4] Q. Peng, H. Li, *Proc. Natl. Acad. Sci. USA* **2008**, *105*, 1885–1890.
- [5] a) C. M. Kaiser, D. H. Goldman, J. D. Chodera, I. Tinoco, C. Bustamante, *Science* **2011**, *334*, 1723–1727; b) K. G. Ugrinov, P. L. Clark, *Biophys. J.* **2010**, *98*, 1312–1320.
- [6] M. Pirchi, G. Ziv, I. Riven, S. S. Cohen, N. Zohar, Y. Barak, G. Haran, *Nat. Commun.* **2011**, *2*, 493.
- [7] K. Chakraborty, M. Chatila, J. Sinha, Q. Shi, B. C. Poschner, M. Sikor, G. Jiang, D. C. Lamb, F. U. Hartl, M. Hayer-Hartl, *Cell* **2010**, *142*, 112–122.
- [8] a) E. A. Shank, C. Cecconi, J. W. Dill, S. Marqusee, C. Bustamante, *Nature* **2010**, *465*, 637–640; b) M. Sikora, M. Cieplak, *Proteins Struct. Funct. Bioinf.* **2011**, *79*, 1786–1799; c) W. Zheng, N. P. Schafer, P. G. Wolynes, *Proc. Natl. Acad. Sci. USA* **2013**, *110*, 1680–1685; d) J. Stigler, M. Rief, *Proc. Natl. Acad. Sci. USA* **2012**, *109*, 17814–17819; e) J. Stigler, F. Ziegler, A. Gieseke, J. C. M. Gebhardt, M. Rief, *Science* **2011**, *334*, 512–516.
- [9] a) J. M. Fernandez, H. Li, *Science* **2004**, *303*, 1674–1678; b) G. Lee, K. Abdi, Y. Jiang, P. Michaely, V. Bennett, P. E. Marszalek, *Nature* **2006**, *440*, 246–249; c) H. Li, Y. Cao, *Acc. Chem. Res.* **2010**, *43*, 1331–1341; d) Y. F. Dufrêne, E. Evans, A. Engel, J. Helenius, H. E. Gaub, D. J. Müller, *Nat. Methods* **2011**, *8*, 123–127; e) E. M. Puchner, H. E. Gaub, *Curr. Opin. Struct. Biol.* **2009**, *19*, 605–614; f) P. M. Williams, S. B. Fowler, R. B. Best, J. L. Toca-Herrera, K. A. Scott, A. Steward, J. Clarke, *Nature* **2003**, *422*, 446–449; g) A. Galera-Prat, A. Gómez-Sicilia, A. F. Oberhauser, M. Cieplak, M. Carrión-Vázquez, *Curr. Opin. Struct. Biol.* **2010**, *20*, 63–69; h) M. S. Bull, R. M. A. Sullan, H. Li, T. T. Perkins, *ACS Nano* **2014**, *8*, 4984–4995; i) U. Hensen, D. J. Müller, *Structure* **2013**, *21*, 1317–1324; j) L. N. Liu, K. Duquesne, F. Oesterhelt, J. N. Sturgis, S. Scheuring, *Proc. Natl. Acad. Sci. USA* **2011**, *108*, 9455–9459; k) M. Brucalè, B. Schuler, B. Samorì, *Chem. Rev.* **2014**, *114*, 3281–3317; l) Z. N. Scholl, W. Yang, P. E. Marszalek, *J. Biol. Chem.* **2014**, *289*, 28607–28618; m) A. J. Jakobi, A. Mashaghi, S. J. Tans, E. G. Huizinga, *Nat. Commun.* **2011**, *2*, 385; n) A. Solanki, K. Neupane, M. T. Woodside, *Phys. Rev. Lett.* **2014**, *112*, 158103; o) J. C. Cordova, A. O. Olivares, Y. Shin, B. M. Stinson, S. Calmat, K. R. Schmitz, M.-E. Aubin-Tam, T. A. Baker, M. J. Lang, R. T. Sauer, *Cell* **2014**, *158*, 647–658; p) A. J. Xu, T. A. Springer, *Proc. Natl. Acad. Sci. USA* **2012**, *109*, 3742–3747.
- [10] H. Dietz, M. Rief, *Proc. Natl. Acad. Sci. USA* **2006**, *103*, 1244–1247.
- [11] M. Bertz, M. Rief, *J. Mol. Biol.* **2008**, *378*, 447–458.
- [12] A. Kedrov, H. Janovjak, K. T. Sapra, D. J. Müller, *Annu. Rev. Biophys. Biomol. Struct.* **2007**, *36*, 233–260.
- [13] E. M. Puchner, A. Alexandrovich, A. L. Kho, U. Hensen, L. V. Schäfer, B. Brandmeier, F. Gräter, H. Grubmüller, H. E. Gaub, M. Gautel, *Proc. Natl. Acad. Sci. USA* **2008**, *105*, 13385–13390.
- [14] A. N. Lupas, M. Gruber in *Advances in Protein Chemistry, Vol. 70* (Eds.: David A. D. Parry, J. M. Squire), Academic Press, New York, **2005**, pp. 37–38.
- [15] a) T. Bornschlöggl, M. Rief, *Langmuir* **2008**, *24*, 1338–1342; b) Y. Gao, G. Sirinakis, Y. Zhang, *J. Am. Chem. Soc.* **2011**, *133*, 12749–12757; c) Z. Xi, Y. Gao, G. Sirinakis, H. Guo, Y. Zhang, *Proc.*

- Natl. Acad. Sci. USA* **2012**, *109*, 5711–5716; d) T. Bornschlöggl, G. Woehlke, M. Rief, *Proc. Natl. Acad. Sci. USA* **2009**, *106*, 6992–6997; e) T. Bornschlöggl, M. Rief, *Phys. Rev. Lett.* **2006**, *96*, 118102.
- [16] M. Chwastyk, A. Galera-Prat, M. Sikora, À. Gómez-Sicilia, M. Carrión-Vázquez, M. Cieplak, *Proteins Struct. Funct. Bioinf.* **2014**, *82*, 717–726.
- [17] W. Lee, X. Zeng, H.-X. Zhou, V. Bennett, W. Yang, P. E. Marszalek, *J. Biol. Chem.* **2010**, *285*, 38167–38172.
- [18] D. Serquera, W. Lee, G. Settanni, P. E. Marszalek, E. Paci, L. S. Itzhaki, *Biophys. J.* **2010**, *98*, 1294–1301.
- [19] W. Lee, X. Zeng, K. Rotolo, M. Yang, C. J. Schofield, V. Bennett, W. Yang, P. E. Marszalek, *Biophys. J.* **2012**, *102*, 1118–1126.
- [20] M. Carrion-Vazquez, P. E. Marszalek, A. F. Oberhauser, J. M. Fernandez, *Proc. Natl. Acad. Sci. USA* **1999**, *96*, 11288–11292.
- [21] M. Aittaleb, R. Rashid, Q. Chen, J. R. Palmer, C. J. Daniels, H. Li, *Nat. Struct. Mol. Biol.* **2003**, *10*, 256–263.
- [22] P. E. Marszalek, Y. F. Dufrêne, *Chem. Soc. Rev.* **2012**, *41*, 3523–3534.
- [23] M. Carrion-Vazquez, A. F. Oberhauser, S. B. Fowler, P. E. Marszalek, S. E. Broedel, J. Clarke, J. M. Fernandez, *Proc. Natl. Acad. Sci. USA* **1999**, *96*, 3694–3699.
- [24] C. He, G. Lamour, A. Xiao, J. Gsponer, H. Li, *J. Am. Chem. Soc.* **2014**, *136*, 11946–11955.
- [25] P. E. Marszalek, H. Lu, H. Li, M. Carrion-Vazquez, A. F. Oberhauser, K. Schulten, J. M. Fernandez, *Nature* **1999**, *402*, 100–103.
- [26] S. K. Wetzel, G. Settanni, M. Kenig, H. K. Binz, A. Plückthun, *J. Mol. Biol.* **2008**, *376*, 241–257.
- [27] A. Steward, J. L. Toca-Herrera, J. Clarke, *Protein Sci.* **2002**, *11*, 2179–2183.
- [28] A. F. Oberhauser, P. E. Marszalek, H. P. Erickson, J. M. Fernandez, *Nature* **1998**, *393*, 181–185.
- [29] E.-L. Florin, M. Rief, H. Lehmann, M. Ludwig, C. Dornmair, V. T. Moy, H. E. Gaub, *Biosens. Bioelectron.* **1995**, *10*, 895–901.
- [30] W. Humphrey, A. Dalke, K. Schulten, *J. Mol. Graphics* **1996**, *14*, 33–38.
- [31] a) A. D. MacKerell, Jr., D. Bashford, M. Bellott, R. Dunbrack, J. Evanseck, M. J. Field, S. Fischer, J. Gao, H. Guo, S. A. Ha, *J. Phys. Chem. B* **1998**, *102*, 3586–3616; b) A. D. MacKerell, Jr., M. Feig, C. L. Brooks, *J. Comput. Chem.* **2004**, *25*, 1400–1415.
- [32] J. C. Phillips, R. Braun, W. Wang, J. Gumbart, E. Tajkhorshid, E. Villa, C. Chipot, R. D. Skeel, L. Kale, K. Schulten, *J. Comput. Chem.* **2005**, *26*, 1781–1802.
- [33] a) J. K. Noel, P. C. Whitford, K. Y. Sanbonmatsu, J. N. Onuchic, *Nucleic Acids Res.* **2010**, *38*, W657–W661; b) C. Clementi, H. Nymeyer, J. N. Onuchic, *J. Mol. Biol.* **2000**, *298*, 937–953.
- [34] H. Lu, B. Isralewitz, A. Krammer, V. Vogel, K. Schulten, *Biophys. J.* **1998**, *75*, 662–671.
- [35] a) H. J. Berendsen, D. van der Spoel, R. van Drunen, *Comput. Phys. Commun.* **1995**, *91*, 43–56; b) E. Lindahl, B. Hess, D. van der Spoel, *J. Mol. Model.* **2001**, *7*, 306–317.